Distorted-wave description of electron momentum spectroscopy for molecules: A demonstration for molecular oxygen

Maomao Gong,[1,*] Yuting Zhang,[1] Xingyu Li ⬥,[1] Song Bin Zhang,[2] Xu Shan ⬥,[1,†] and Xiangjun Chen ⬥[1,‡]

[1]*Hefei National Laboratory for Physical Sciences at Microscale and Department of Modern Physics, University of Science and Technology of China, Hefei 230026, China*

[2]*School of Physics and Information Technology, Shaanxi Normal University, Xi'an 710119, China*

An accurate description of electron momentum spectroscopy (EMS) for molecular targets remains unresolved since its advent several decades ago. Here, we report a multicenter three-distorted-wave calculation of electron momentum profiles for molecules. The accuracy of the calculation method is demonstrated by an EMS study on oxygen molecules at various electron impact energies ranging from 608 to 1808 eV. The calculations are in excellent agreement with the experiment for all the observed valence orbitals, especially the "turn-up" at zero momentum for the $1\pi_g$ orbital as well as the intensities at large momentum up to 6.0 a.u. where the cross sections are extremely low.

I. INTRODUCTION

.Since the pioneering works of Camilloni *et al.* [1] and Weigold *et al.* [2], electron momentum spectroscopy (EMS) has been developed into a robust probe for imaging orbital-specific electron density distributions in momentum space from simple atoms and molecules [3–7] to large biomolecules [8]. Benefited from the recently developed high-sensitivity angle- and energy-dispersive multichannel technique [9–12], EMS exhibits great potential in investigating the electronic structures of molecules in excited states [13,14], in the molecular frame [15,16], as well as retrieving molecular geometry from multicenter interference [17–19]. Besides the time-resolved EMS [11,12], which aims at measuring in real time the momentum distributions of electrons, bound in a transient, evolving system, Sendai's group has extended such a time-resolved technique to time-resolved atomic momentum spectroscopy [20], trying to obtain a series of snapshot microscopic views of a gas-phase photochemical reaction.

EMS, or binary $(e, 2e)$ spectroscopy, is an electron-impact ionization experiment near the Bethe ridge with keV incident electrons. The use of the $(e, 2e)$ reaction as a probe for orbital imaging requires a good understanding of the probe. The well-established EMS theory consists of a series of approximations including binary encounter, weak coupling, plane-wave impulse, as well as target Hartree-Fock (HF) or target Kohn-Sham (KS) approximations [21]. Within these approximations the measured $(e, 2e)$ triple differential cross section (TDCS) is proportional to the spherically averaged modulus square of the electron wave function of an ionized

orbital in the momentum space or the electron momentum profile (EMP). The plane-wave impulse approximation (PWIA) is usually adequate to describe EMP shapes in momentum regions less than 1 a.u. [22], but underestimates the high-momentum cross sections. For atoms, this can be accounted for by the distorted-wave Born [23,24] or the distorted-wave impulse approximations [24] (DWBA or DWIA), in which the continuum electrons are described by the distorted waves calculated in a suitable potential, rather than by plane waves. More interestingly, for atomic d orbitals [25,26], PWIA-unpredicted nonzero intensity at zero momentum (usually referred to as "turn-up") was observed and can readily be reproduced by the distorted-wave calculations. This "turn-up" was also observed for some molecular orbitals [26–28], especially for π^* orbitals. Both the distorted-wave effect and molecular vibrational effect may contribute to this turn-up. The influence of the vibrational motion can be analyzed by harmonic analytical quantum mechanical calculations [29] or by molecular dynamic simulations [30]. However, the distorted-wave calculation at the EMS condition remains unresolved since the invention of the EMS technique several decades ago. Ren *et al.* [27] explored the distorted-wave effect on the turn-up for a $1b_{3g}$ orbital of ethylene. Their investigation was based on the fact that the discrepancy between the measured TDCS and the PWIA calculations decreases with an increase of the electron impact energies both at low- and high-momentum regions. A similar behavior was also observed for the highest occupied molecular orbital (HOMO) of oxygen (O_2) which is a typical π^* orbital [28]. But the confirmation of the distorted-wave effect needs accurate distorted-wave calculations.

Very recently, we have developed a multicenter three-distorted-wave (MCTDW) method [31] aiming at calculating $(e, 2e)$ fully differential cross sections for a molecular target. An overall agreement with experiment has been achieved in predicting three-dimensional electron-impact-ionization

---

*gongmm@ustc.edu.cn
†xshan@ustc.edu.cn
‡xjun@ustc.edu.cn

dynamics at low energy [31,32]. But the rapidly increased computational cost resulting from the big number of partial waves of continuum wave functions and a large number of molecular orientations prevent it from being applied to the EMS condition. In this paper, we have improved the algorithm of the MCTDW by using a parallel program and successfully included a large number of partial waves. Therefore, the distorted-wave calculation of EMP for molecular targets becomes practical. Here, as a demonstration, an EMS investigation on the O_2 molecule is reported. The experiments are performed using a high-sensitivity EMS apparatus [9] at three different electron impact energies of 608, 1208, and 1808 eV. The measured EMPs for all the observed valence orbitals of O_2 are well reproduced by the MCTDW calculations within a large momentum range from the origin to 6 a.u. for all three impact energies, especially for the HOMO $1\pi_g$, where the turn-ups at the origin are accurately described by the MCTDW method.

II. THEORETICAL AND EXPERIMENTAL METHODS

EMS is based on an $(e, 2e)$ experiment in which an electron from a target is knocked out by a high-energy incident electron, and the residual ion acts as a spectator. From the energy and momentum conservation, the binding energy ε_f and the momentum $\vec{p}$ of the target electron are given by

$$\varepsilon_f = E_i - E_s - E_e, \tag{1}$$

$$\vec{p} = \vec{k}_s + \vec{k}_e - \vec{k}_i, \tag{2}$$

where $(E_i, \vec{k}_i)$, $(E_s, \vec{k}_s)$, and $(E_e, \vec{k}_e)$ represent energies and momentum vectors of the incident, scattered, and ejected electrons, respectively.

In the MCTDW method [31], for a randomly oriented molecular target, the TDCS can be expressed as

$$\frac{d^3\sigma}{d\Omega_e d\Omega_s dE_s} = \frac{1}{(2\pi)^5} \frac{k_s k_e}{k_i} \frac{1}{8\pi^2} \int |T_{fi}(\Omega)|^2 d\Omega, \tag{3}$$

Here, we show the ionization amplitude

$$T_{fi}(\Omega) = \left\langle \mathcal{F}_e^{(-)}(\vec{k}_e; \mathcal{R}_\Omega^{-1}\vec{r}_1) \mathcal{F}_s^{(-)}(\vec{k}_s; \mathcal{R}_\Omega^{-1}\vec{r}_0) \right| \frac{1}{|\vec{r}_0 - \vec{r}_1|}$$
$$- \frac{1}{N} \sum_n \frac{Z_n}{|\vec{r}_0 - \vec{R}_n|} \left| \varphi_\alpha(\mathcal{R}_\Omega^{-1}\vec{r}_1) \mathcal{F}_i^{(+)}(\vec{k}_i; \mathcal{R}_\Omega^{-1}\vec{r}_0) \right\rangle, \tag{4}$$

where $\mathcal{F}_e^{(-)}$, $\mathcal{F}_s^{(-)}$, and $\mathcal{F}_i^{(+)}$ are multicenter distorted waves for the ejected, scattered, and incident electrons, respectively, which are solved in the multicenter ionic (or neutral) molecular potentials [31]. φ_α is the Dyson orbital to be ionized, which is usually approximated by the Hartree-Fock or Kohn-Sham orbital. The molecular orientation is defined by the Euler angle $\Omega = (\alpha, \beta, \gamma)$. $\mathcal{R}_\Omega^{-1}$ represents the rotation operator. $\vec{r}_0$ and $\vec{r}_1$ are the coordinates of the projectile and target active electrons, respectively. $\vec{R}_n$ is the position of the nth nucleus and Z_n indicates its charge. N is the total electron number of the molecular system.

The MCTDW can be simplified to PWIA if the multicenter continuum distorted waves are replaced by the plane waves,

$$\frac{d^3\sigma}{d\Omega_e d\Omega_s dE_s} = \frac{1}{(2\pi)^5} \frac{k_s k_e}{k_i} \frac{1}{8\pi^2} \frac{(4\pi)^2}{|\vec{k}_i - \vec{k}_s|^4}$$
$$\times \int \left| \int e^{i(\vec{k}_i - \vec{k}_s - \vec{k}_e)\cdot\vec{r}_1} \varphi_\alpha(R_\Omega^{-1}\vec{r}_1) d\vec{r}_1 \right|^2 d\Omega$$
$$\propto \int d\Omega_p |\varphi_\alpha(\vec{p})|^2. \tag{5}$$

In the MCTDW model [31], the sudden approximation is adopted, and the final ion configuration is actually a one-hole state $\bar{\alpha}$ corresponding to orbital α. If taking into account electron correlation, in the weak-coupling approximation, the final ion state f can be described by an expansion containing the single-hole state $\bar{\alpha}$. The probability of finding a one-hole configuration in the final ion state is called the spectroscopic factor S_f^α (or pole strength), which is not included in the MCTDW and PWIA calculations.

In the present work, the position space bound wave functions are calculated by the density-functional theory method employing the Becke three-parameter Lee-Yang-Parr (B3LYP) hybrid functional [33,34] and augmented correlation-consistent polarized valence triple zeta (aug-cc-pVTZ) basis set [35] using the GAUSSIAN 09 [36] program.

The experiments are performed at three incident electron energies, $E_i = 608$, 1208, and 1808 eV, using a high-sensitivity EMS apparatus employing symmetric noncoplanar geometry [9,37]. Briefly, an incident electron from the electron gun impacts with a gas-phase O_2 molecule and knocks out an orbital electron from it. The two outgoing electrons with equal polar angles ($\theta_s = \theta_e = 45°$) and energies ($E_s = E_e$) pass through a $90°$ sector spherical electrostatic analyzer with a 2π azimuthal range, and are detected in coincidence by a position-sensitive detector composed of two microchannel plates in a chevron configuration followed by a delay line anode (HEX 120 from RoentDek Handels GmbH). In this kinematics, the magnitude of the momentum in Eq. (2) can be expressed as

$$p = \sqrt{\left(\sqrt{2}k_s - k_i\right)^2 + \left[\sqrt{2}k_s \sin(\phi/2)\right]^2}, \tag{6}$$

where ϕ is the relative azimuthal angle between the two outgoing electrons. The instrumental angular and energy resolutions are determined to be $\Delta\theta = \pm 0.8°$, $\Delta\phi = \pm 2.0°$, and ~ 1.2 eV, respectively, by measuring Ar $3p$ before and after the O_2 molecule experiment.

III. RESULTS AND DISCUSSION

Figure 1(a) shows a two-dimensional (2D) electron density map for O_2 measured at $E_i = 1208$ eV, which is the $(e, 2e)$ TDCS as functions of the binding energy and relative azimuthal angle ϕ (i.e., the momentum of the orbital electron) and contains all the information on the binding energy spectra (BES), electron momentum distributions, and symmetries for various ionic states. O_2 belongs to the $D_{\infty h}$ point group and its open-shell ground-state electronic configuration is $(1\sigma_g)^2(1\sigma_u)^2(2\sigma_g)^2(2\sigma_u)^2(3\sigma_g)^2(1\pi_u)^4(1\pi_g)^2$. By integrating the 2D map over all measured azimuthal angles, the total
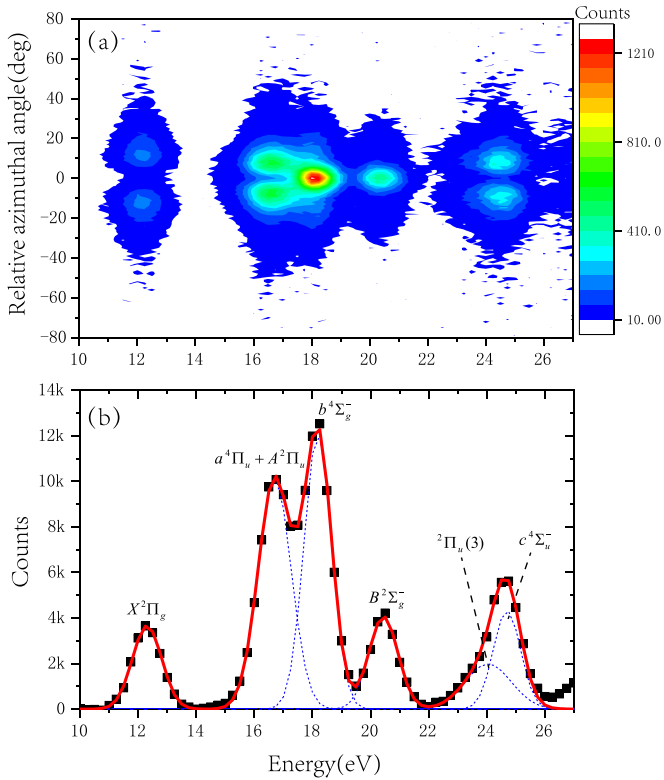
FIG. 1. (a) Two-dimensional energy and relative azimuthal angle (ϕ) density map at $E_i = 1208$ eV for the O$_2$ molecule. (b) Total binding energy spectrum.

BES is obtained, which is shown in Fig. 1(b). The measured binding energy range is from 10 to 27 eV, covering seven ionic states. Six Gaussian functions are invoked to fit the BES, as shown by blue dotted lines in Fig. 1(b). The positions of the Gaussian peaks are referred to the photoelectron spectroscopy (PES) [38]. The widths of the peaks are the Franck-Condon widths folded with the instrumental energy resolution [1.2 eV in full width at half maximum (FWHM)]. The red solid line represents the summation. The first peak at 12.3 eV corresponds to the $X^2\Pi_g$ ground ionic state from the ionization of HOMO $1\pi_g$. Removal of an electron from the $1\pi_u$ orbital leads to $a^4\Pi_u$, $A^2\Pi_u$ ionic states and a satellite state $^2\Pi_u(3)$. Due to the limited instrumental energy resolution, we use one Gaussian function at 17.0 eV to fit $a^4\Pi_u$, $A^2\Pi_u$ and one at 24.0 eV to fit $^2\Pi_u(3)$. Gaussian functions at 18.2 and 20.4 eV represent the $b^4\Sigma_g^-$ and $B^2\Sigma_g^-$ ionic states from the $3\sigma_g$ orbital, while the one at 24.7 eV corresponds to the ionic state $c^4\Sigma_u^-$ from the ionization of the $2\sigma_u$ orbital.

The experimental momentum profiles (XMPs) for each ionization peak are obtained by deconvoluting the BES at each azimuthal angle and plotting the area of the fitted Gaussian peaks as a function of momentum p which is calculated from the azimuthal angle ϕ according to Eq. (6). The XMPs for the HOMO $1\pi_g$ orbital ($X^2\Pi_g$ ionic state) at 608, 1208, and 1808 eV impact energies are shown in Fig. 2. The electron density map of HOMO is also displayed in the figure. The experimental results are compared with theoretical momentum profiles (TMPs) calculated by MCTDW, as well as PWIA. To make them comparable with experiments, TMPs are folded
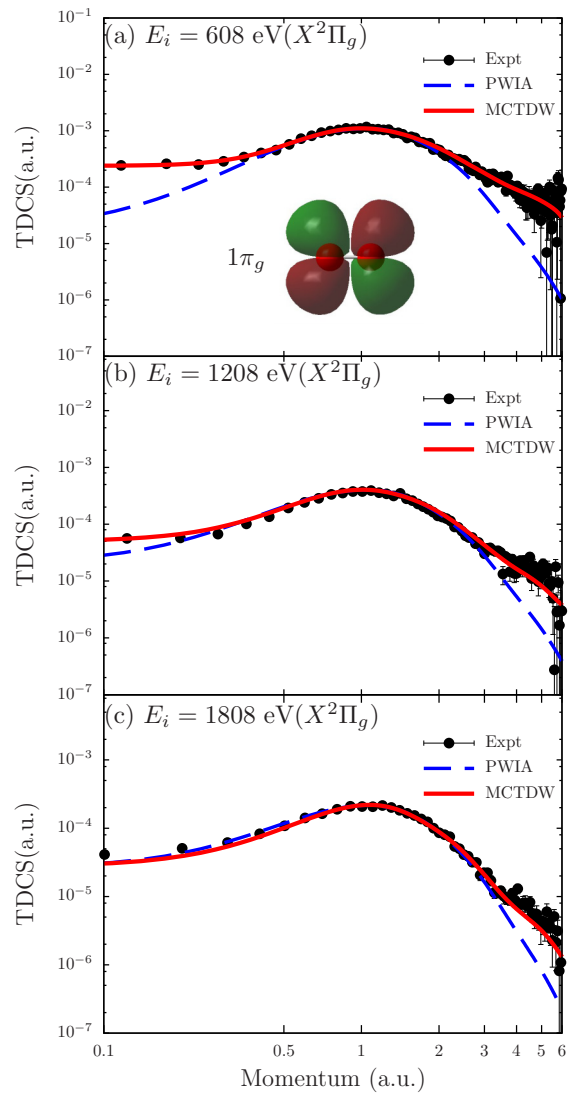

FIG. 2. The electron momentum profiles for HOMO of the O$_2$ molecule at various collision energies: (a) 608 eV, (b) 1208 eV, and (c) 1808 eV. The black circles are the present experimental data. The solid red and dashed blue lines are the calculation results of the MCTDW and PWIA models for the $X^2\Pi_g$ ionic state, respectively.

with the instrumental angular resolutions using the Gaussian weighted planar grid method [39]. The XMPs are normalized to the TMPs of MCTDW and the obtained normalization factors are then invoked for other ionic states, as well as PWIA calculations. PWIA-TMPs therefore should be scaled by a factor to height normalized to the experiment. It can be seen in Figs. 2(a)–2(c) that the scaled PWIA calculations clearly underestimate the XMPs in both low- and high-momentum regions and the discrepancies between them decrease with the increase of the electron impact energies, suggesting the distorted-wave effect.

The occurrence of distorted-wave effects at higher momenta can be readily understood since this region of the electron momentum profile involves significant penetration by the incoming electron (and thus also by the outgoing electrons) into the smaller r region, near the nucleus [26]. Such an effect at the higher momenta becomes so weak at 1808 eV

impact energy that the PWIA is adequate to describe XMPs in a momentum region less than 3 a.u. In a recent combined experimental and theoretical study of EMS of sulfur hexafluoride [40], the molecular three-body distorted-wave approach was tentatively used to calculate the TMPs of the $5a_{1g}$ orbital and showed the energy-dependent features qualitatively with poor agreement in a momentum region larger than 0.6 a.u. The present MCTDW calculations, however, precisely reproduce the XMPs (even shown in logarithmic scale at large momenta up to 6.0 a.u.) at all three impact energies.

Regardless of momentum resolution, the PWIA calculation predicts zero intensity at $p = 0$ a.u., while the obvious turn-up has been observed in the XMPs as shown in Fig. 2. The discrepancies between PWIA calculations and experiments significantly decrease as the electron impact energy increases. For atomic d orbitals [25,26], this turn-up can be reproduced by the distorted-wave calculations. Brion *et al.* [26] ascribed these distortion effects at low momenta to a high-l effect and the even-parity nature of atomic d orbitals. As the momentum corresponds to the gradient of the wave function in the position space [26], for atomic d orbitals, low momenta (i.e., low gradient) can contribute to the electron density in the near nuclear region, leading to the strong distorted-wave effect near the nucleus in the low-momentum region. Molecular orbitals of dominantly atomic d character would also be expected to exhibit significant distortion effects in their $(e, 2e)$ cross sections (i.e., momentum profiles) at low momenta, as observed in the case of the HOMO $1\pi_g$ orbital of the O_2 molecule in the present work. These distortion effects can now be well reproduced by the present MCTDW calculations.

To investigate the generality of the MCTDW method, we present theoretical and experimental momentum profiles of O_2 for other ionic states at $E_i = 1208$ eV, as shown in Figs. 3(a)–3(e). Considering the pole strength of the ionic states, the MCTDW and PWIA calculations must be multiplied by proper factors (the relative pole strength) to achieve the best visual fit with experiments. Obviously, the MCTDW calculations well reproduce the experiments for all the ionic states, especially in the large momentum region, where the cross sections are extremely low.

For the open-shell system of the oxygen molecule, as it was described by Rolke *et al.* [41], one must multiply relative intensity factors F for a given ionic state to construct the spin-restricted TMPs, and F includes the degeneracy and occupancy of the initial orbital. Thus, the EMS cross section for an ionic state can be written as

$$\sigma_{\text{EMS}} = F S_f^\alpha \frac{d^3\sigma}{d\Omega_e d\Omega_s dE_s}. \tag{7}$$

The relative intensity factors F for ionic states $X^2\Pi_g$, $a^4\Pi_u$, $A^2\Pi_u$, $b^4\Sigma_g^-$, $B^2\Sigma_g^-$, and $c^4\Sigma_u^-$ are 2, 8/3, 4/3, 4/3, 2/3, and 4/3 [41], respectively, which are already included in the MCTDW and PWIA TMPs in the figures. The pole strength S_f^α for each ionic state can be obtained from Eq. (7). The relative pole strengths of the MCTDW calculation for ionic states $X^2\Pi_g$, $a^4\Pi_u + A^2\Pi_u$, $b^4\Sigma_g^-$, $B^2\Sigma_g^-$, $^2\Pi_u(3)$, and $c^4\Sigma_u^-$ are 1.0, 1.3, 1.2, 0.9, 0.75, and 0.7, respectively. For the
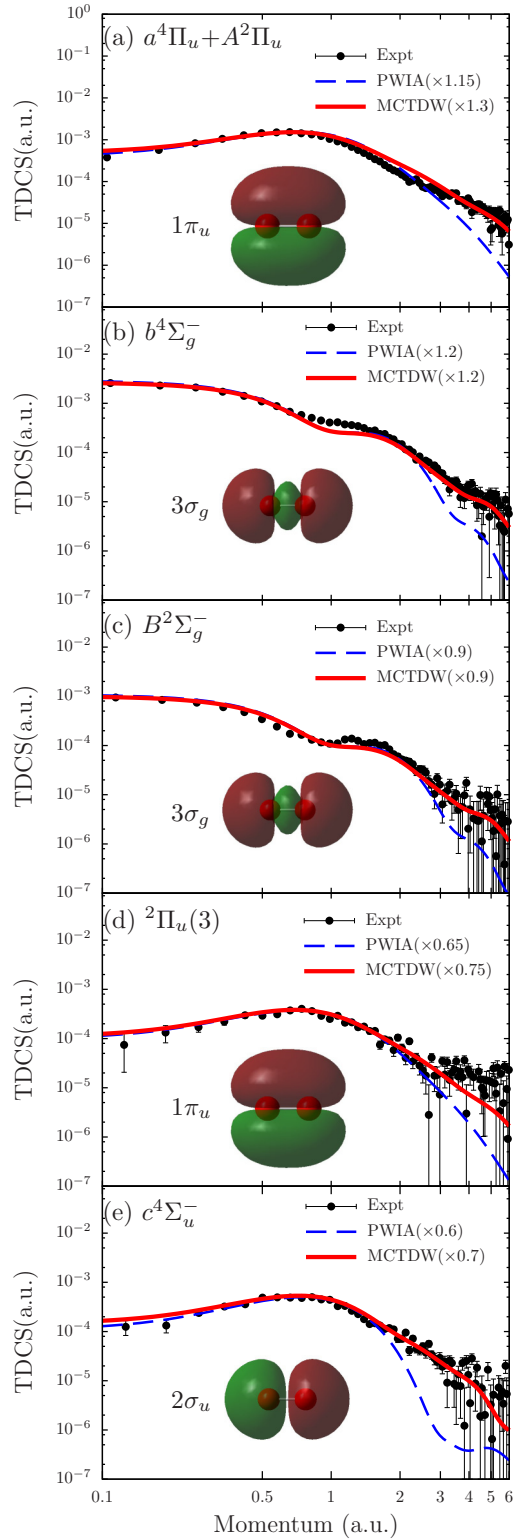

FIG. 3. The electron momentum profiles for ionic states except $X^2\Pi_g$ at $E_i = 1208$ eV: (a) sum of $a^4\Pi_u$ and $A^2\Pi_u$ states, (b) $b^4\Sigma_g^-$ state, (c) $B^2\Sigma_g^-$ state, (d) $^2\Pi_u(3)$ state, and (e) $c^4\Sigma_u^-$ state. The black circles are the present experimental data. The solid red and dashed blue lines are the calculation results of the MCTDW and PWIA models, respectively. The multiplied factors for the MCTDW and PWIA calculations are also displayed in the legends.

present PWIA calculations, they are 1.0, 1.15, 1.2, 0.9, 0.65, and 0.6.

IV. SUMMARY

In summary, the distorted-wave calculation at the EMS condition for molecular target has become practical by employing the MCTDW method. The accuracy of the method has been demonstrated by an EMS investigation on the O_2 molecule. The experiments are performed at three different electron impact energies of 608, 1208, and 1808 eV. The XMPs for all the ionic states from the single ionization of the observed valence orbitals of O_2 are well reproduced by the MCTDW calculations within a large momentum range from 0 to 6 a.u. for broad impact energies. More specifically, the turn-up at the origin for the HOMO $1\pi_g$, as well as the intensities in the large momentum region from 3.0 to 6.0 a.u. where the cross sections are extremely low, are precisely described by the present MCTDW method. Ideally, if one wants to detect the undisturbed momentum distribution of a bound electron orbital, the electron impact energy should be high enough to ensure that the plane-wave approximation holds. However, in the practical experiment, the impact energy is usually limited.

So the distorted-wave effect in the scattering process cannot be avoided. Therefore, to develop a theoretical method considering the distorted-wave effect is of importance. This MCTDW method may also have potential applications in laser-induced inelastic scattering approaches, based on the nonsequential double-ionization process driven by an intense femtosecond laser field [42]. In the strong-field rescattering model, the recolliding electron may also inelastically scatter off the parent ion, with a second electron being kicked out. This corresponds to the conventional $(e, 2e)$ process.

[1] R. Camilloni, A. G. Guidoni, R. Tiribelli, and G. Stefani, Phys. Rev. Lett. **29**, 618 (1972).

[2] E. Weigold, S. T. Hood, and P. J. O. Teubner, Phys. Rev. Lett. **30**, 475 (1973).

[3] I. E. McCarthy, A. Ugbabe, E. Weigold, and P. J. O. Teubner, Phys. Rev. Lett. **33**, 459 (1974).

[4] J. P. D. Cook, J. Mitroy, and E. Weigold, Phys. Rev. Lett. **52**, 1116 (1984).

[5] Y. Zheng, I. E. McCarthy, E. Weigold, and D. Zhang, Phys. Rev. Lett. **64**, 1358 (1990).

[6] S. T. Hood, E. Weigold, I. E. McCarthy, and P. J. O. Teubner, Nat. Phys. Sci. **245**, 65 (1973).

[7] S. Dey, I. E. McCarthy, P. J. O. Teubner, and E. Weigold, Phys. Rev. Lett. **34**, 782 (1975).

[8] Y. Zheng, J. J. Neville, and C. E. Brion, Science **270**, 786 (1995).

[9] Q. Tian, K. Wang, X. Shan, and X. Chen, Rev. Sci. Instrum. **82**, 033110 (2011).

[10] M. Yamazaki, H. Satoh, M. Ueda, D. B. Jones, Y. Asano, N. Watanabe, A. Czasch, O. Jagutzki, and M. Takahashi, Meas. Sci. Technol. **22**, 075602 (2011).

[11] M. Yamazaki, Y. Kasai, K. Oishi, H. Nakazawa, and M. Takahashi, Rev. Sci. Instrum. **84**, 063105 (2013).

[12] Y. Tang, X. Shan, Z. Liu, S. Niu, E. Wang, and X. Chen, Rev. Sci. Instrum. **89**, 033101 (2018).

[13] M. Yamazaki, K. Oishi, H. Nakazawa, C. Zhu, and M. Takahashi, Phys. Rev. Lett. **114**, 103005 (2015).

[14] M. Yamazaki, Y. Tang, and M. Takahashi, Phys. Rev. A **94**, 052509 (2016).

[15] M. Takahashi, N. Watanabe, Y. Khajuria, Y. Udagawa, and J. H. D. Eland, Phys. Rev. Lett. **94**, 213202 (2005).

[16] S. Bellm, J. Lower, E. Weigold, and D. W. Mueller, Phys. Rev. Lett. **104**, 023202 (2010).

[17] N. Watanabe, X. J. Chen, and M. Takahashi, Phys. Rev. Lett. **108**, 173201 (2012).

[18] Z. Zhang, X. Shan, T. Wang, E. Wang, and X. Chen, Phys. Rev. Lett. **112**, 023204 (2014).

[19] E. Wang, X. Shan, Q. Tian, J. Yang, M. Gong, Y. Tang, S. Niu, and X. Chen, Sci. Rep. **6**, 39351 (2016).

[20] M. Yamazaki, M. Hosono, Y. Tang, and M. Takahashi, Rev. Sci. Instrum. **88**, 063103 (2017).

[21] E. Weigold and I. E. McCarthy, *Electron Momentum Spectroscopy* (Kluwer Academic/Plenum Press, New York, 1999).

[22] M. Takahashi, Bull. Chem. Soc. Jpn. **82**, 751 (2009).

[23] I. McCarthy, Aust. J. Phys. **48**, 1 (1995).

[24] D. H. Madison, R. V. Calhoun, and W. N. Shelton, Phys. Rev. A **16**, 552 (1977).

[25] M. J. Brunger, S. W. Braidwood, I. E. McCarthy, and E. Weigold, J. Phys. B: At. Mol. Opt. Phys. **27**, L597 (1994).

[26] C. E. Brion, Y. Zheng, J. Rolke, J. J. Neville, I. E. McCarthy, and J. Wang, J. Phys. B: At. Mol. Opt. Phys. **31**, L223 (1998).

[27] X. G. Ren, C. G. Ning, J. K. Deng, S. F. Zhang, G. L. Su, F. Huang, and G. Q. Li, Phys. Rev. Lett. **94**, 163201 (2005).

[28] C. G. Ning, X. G. Ren, J. K. Deng, G. L. Su, S. F. Zhang, and G. Q. Li, Phys. Rev. A **73**, 022704 (2006).

[29] N. Watanabe, M. Yamazaki, and M. Takahashi, J. Chem. Phys. **137**, 114301 (2012).

[30] F. Morini, M. S. Deleuze, N. Watanabe, and M. Takahashi, J. Chem. Phys. **142**, 094308 (2015).

[31] M. Gong, X. Li, S. B. Zhang, S. Niu, X. Ren, E. Wang, A. Dorn, and X. Chen, Phys. Rev. A **98**, 042710 (2018).

[32] M. Gong, Z. Wang, X. Li, S. B. Zhang, and X. Chen, J. Phys. B: At. Mol. Opt. Phys. **54**, 015206 (2021).

[33] A. D. Becke, J. Chem. Phys. **98**, 5648 (1993).

[34] C. Lee, W. Yang, and R. G. Parr, Phys. Rev. B **37**, 785 (1988).

[35] T. H. Dunning, Jr., J. Chem. Phys. **90**, 1007 (1989).

[36] M. J. Frisch, G. W. Trucks, H. B. Schlegel, G. E. Scuseria, M. A. Robb, J. R. Cheeseman, G. Scalmani, V. Barone, G. A. Petersson, H. Nakatsuji *et al.*, *Gaussian 09, Revision A.02* (Gaussian, Inc., Wallingford, CT, 2016).

[37] Y. Tang, X. Shan, S. Niu, Z. Liu, E. Wang, N. Watanabe, M. Yamazaki, M. Takahashi, and X. Chen, J. Phys. Chem. A **121**, 277 (2017).

[38] P. Baltzer, B. Wannberg, L. Karlsson, M. Carlsson Göthe, and M. Larsson, Phys. Rev. A **45**, 4374 (1992).

[39] P. Duffy, M. E. Cassida, C. Brion, and D. Chong, Chem. Phys. **159**, 347 (1992).

[40] X. Wang, S. Xu, C. Ning, O. Al-Hagan, P. Hu, Y. Zhao, Z. Xu, J. Deng, E. Wang, X. Ren, A. Dorn, and D. Madison, Phys. Rev. A **97**, 062704 (2018).

[41] J. Rolke, Y. Zheng, C. Brion, Y. Wang, and E. Davidson, Chem. Phys. **230**, 153 (1998).

[42] W. Quan, X. L. Hao, X. Q. Hu, R. P. Sun, Y. L. Wang, Y. J. Chen, S. G. Yu, S. P. Xu, Z. L. Xiao, X. Y. Lai, X. Y. Li, W. Becker, Y. Wu, J. G. Wang, X. J. Liu, and J. Chen, Phys. Rev. Lett. **119**, 243203 (2017).